Impaired brainstem and thalamic high frequency oscillatory EEG activity in migraine between attacks

Camillo Porcaro[1,2,3], Giorgio Di Lorenzo[4,5], Stefano Seri[6], Francesco Pierelli[7], Franca Tecchio[1,8], Gianluca Coppola[9]

[1] LET'S-ISTC-CNR, Ospedale Fatebenefratelli, Isola Tiberina, Rome, Italy

[2] Institute of Neuroscience, Newcastle University, Medical School, Newcastle upon Tyne, UK

[3] Department of Information Engineering, Università Politecnica delle Marche, Ancona, Italy

[4] Laboratory of Psychophysiology, Psychiatric Chair, Department of Systems Medicine, University of Rome "Tor Vergata", Rome, Italy

[5] Psychiatry and Clinical Psychology Unit, Department of Neurosciences, Fondazione Policlinico "Tor Vergata", Rome, Italy

[6] The Wellcome Trust Laboratory for MEG Studies, School of Life and Health Sciences, Aston University, Birmingham, UK

[7] Sapienza University of Rome Polo Pontino, Latina & IRCCS Neuromed, Pozzilli (IS), Italy

[8] Unit of Neuroimaging, IRCCS San Raffaele Pisana, Rome, Italy

[9] G.B. Bietti Foundation IRCCS, Department of Neurophysiology of Vision and Neurophthalmology, Rome, Italy

Corresponding author:

Camillo Porcaro
LET'S-ISTC-CNR
Fatebenefratelli Hospital - Isola Tiberina
00186 Rome, Italy
Tel: +39 06 6837300
Fax: +39 06 6837360
E-mail: camillo.porcaro@istc.cnr.it

Abstract

Introduction: We investigated whether interictal thalamic dysfunction in migraine without aura (MO) patients is a primary determinant or the expression of its functional disconnection from proximal or distal areas along the somatosensory pathway.

Methods: Twenty MO patients and twenty healthy volunteers (HV) underwent an electroencephalographic (EEG) recording during electrical stimulation of the median nerve at the wrist. We used Functional Source Separation algorithm to extract four functionally constrained nodes (brainstem, thalamus, primary sensory radial, and primary sensorymotor tangential parietal sources) along the somatosensory pathway. Two digital filters (1-400 Hz and 450-750 Hz) were applied in order to extract low- (LFO) and high- frequency (HFO) oscillatory activitiy from the broadband signal.

Results: Compared to HV, patients presented significantly lower brainstem (BS) and thalamic (Th) HFO activation bilaterally. No difference between the two cortical HFO as well as in LFO peak activations between the two groups was seen. The age of onset of the headache was positively correlated with HFO power in the right brainstem and thalamus.

Conclusions: This study provides evidence for complex dysfunction of brainstem and thalamocortical networks under the control of genetic factors that might act by modulating the severity of migraine phenotype.

Key words: High Frequency Oscillations (HFOs), Functional Source Separation (FSS), Migraine, Brainstem, Thalamus, Electroencephalography (EEG).

Introduction

In recent years the thalamus has received growing attention as a key brain structure in migraine pathophysiology, not just as a relay station but also as a site of multisensory integration, being profoundly involved in its clinical and neurophysiological expression. Evidence from animal models have indicated that a temporary sensitization of third-order thalamic neurons receiving convergent input from the dura, the periorbital skin, and from more distal cutaneous regions play a critical role in the clinical manifestation of central sensitization – allodynia - beyond the original referred ictal headache region (1). Abnormal modulatory activity of the lateral geniculate complex, the thalamic relay of the visual system, might be involved in the process responsible for migraine-associated symptomology, such as photophobia (2). The anatomical correlates of this thalamic dysfunction are only recently beginning to be understood (3,4). However, as the thalamus is part of interconnected cortical and subcortical networks, neurophysiological measures offer a unique opportunity to investigate whether patients with migraine present a primary thalamic dysfunction between attacks.

Scalp responses to peripheral electrical stimulation (somatosensory evoked responses or SSEP) have been used to measure the influence of arousal systems on cortical somatosensory input processing. Studies have identified that SSEP are characterised by low-frequency oscillatory brain activity (LFOs), and by high-frequency bursts of wavelets (high-frequency oscillations, HFOs) that are more evident in the frontal-parietal region contralateral to the stimulated side (5). SSEPs multichannel dipole source analysis has demonstrated four levels of sequential activation of HFOs: the first located in the brainstem, followed by the thalamus, the third located tangentially over the parietal area 3b, and the fourth radially oriented over the sensorimotor associative area (5–7). This geometry of somatosensory pathway sources was recently confirmed in studies that used a novel approach called Functional Source Separation (FSS) (8). This method identifies cerebral sources on the basis of their functional behavior instead of their anatomical position. Allowing the functional characterization of the oscillatory patterns of four nodes of the primary somatosensory pathway, localized respectively in the brain stem, the ventral posterior lateral nucleus of the thalamus, and within the primary sensorimotor cortex (9,10).

In the last decade, several HFO studies have assessed thalamic/thalamocortical activity in patients with migraine using the classical single channel approach, and allowed measurement of the activity of thalamic and primary cortical nodes only, with some limitations in the degree of spatial accuracy. These studies have reported that the activity of the high-frequency oscillatory somatosensory thalamo-cortical connections is reduced interictally in migraine (11,12), especially when associated

with a worsening in the clinical course of the disease (13,14). To the best of our knowledge, there are no somatosensory HFO studies using multichannel EEG associated with FSS procedures to extract the functional activation of the signal generated at each of the sub-cortical (brainstem and thalamus) and cortical (early primary parietal area and late sensorimotor area) neuronal nodes. Biochemical (15) and neuroimaging (16) studies have indicated that brainstem monoaminergic transmission is altered in migraine, and that this may abnormally modulate preactivation levels and signal-to-noise ratio in cortical and thalamocortical neurons. Moreover, maladaptive responses of cortical neurones have been described in patients with migraine during direct cortical repetitive transcranial magnetic stimulation (rTMS). This finding led some authors to speculate that a primary cortical dysfunction could down-regulate thalamic activity via cortico-subcortical feedback loops (17). This body of evidence led us to explore in interictal migraine if the thalamus is the primary site of the dysfunction or whether the thalamic dysfunction occurs secondary to its functional disconnection from brain areas located proximally or distally along the somatosensory pathway and, if the severity of abnormal thalamic function correlated with clinical features of migraine.

Material and methods

Subjects

We recruited 20 consecutive patients attending the headache clinic of "Sapienza" University of Rome Polo Pontino, Latina (Italy) diagnosed with episodic migraine without aura (ICHD IIIbeta). Potential participants were identified during their first visit, and were asked if they consented to participate in the study, which was approved by the University Ethics Committee. The study complied with the principles set out in the WMA Declaration of Helsinki - Ethical Principles for Medical Research Involving Human Subjects.

Inclusion criteria were as follows: no history of other neurological diseases, systemic hypertension, diabetes or other metabolic disorders, connective or autoimmune diseases or any other type of primary or secondary headache. Patients had uni/bilateral migraine headaches, but not fixed pain on the same side. In order to avoid confounding effects of pharmacologic treatment on the EEG signal, no preventive anti-migraine drugs were allowed during the 3 months preceding the brain electrical activity recording. Patients were recorded during the interictal period, defined as absence of migraine attacks for at least three days before and after the recording session.

We also recruited as controls 20 healthy volunteers (HV) from medical school students and healthcare professionals of comparable age and gender distribution; they had no personal or familial

history (1st or 2nd degree relatives) of migraine and no detectable medical condition. All recruited subjects were right-handed. To avoid variability due to hormonal changes, women were recorded outside their pre-menstrual or menstrual periods. All recording sessions were performed in the afternoon between 3.00 and 6.00 p.m. None of the recruited subjects had sleep deprivation or alcohol consumption the day preceding the scans. Caffeinated beverages were not allowed on the day of the recording.

Data acquisition

All recordings were made at the Laboratory of Psychophysiology of the Psychiatric Clinic, Department of Systems Medicine of University of Rome "Tor Vergata", Rome (Italy). Subjects were comfortably sat on a chair in an illuminated room and asked to stay with eyes open, orienting their gaze to a fixed point and their attention to the stimulated hand. Stable levels of arousal were further monitored using the on-line EEG signal. Somatosensory evoked potentials were elicited after electrical stimulation of the median nerve at the wrist using a Digitimer DS7A device (Digitimer Ltd, UK) with constant-current square wave pulses (0.2 ms width, cathode proximal), stimulus intensity set at 1.5 times the motor threshold, and at repetition rate of 4.4/s. For each subject, two series of one-thousand sweeps were collected, one for each side. The stimulus side sequence was chosen randomly.

EEG was acquired form 39 electrodes using a pre-cabled electrode cap (Bionen, Florence, Italy) from the positions FP1, FPz, FP2, AF4, AF3, F7, F3, Fz, F4, F8, FC5, FC3, FC1, FCz, FC2, FC4, FC6, T3, C3, Cz, C4, T4, CP5, CP3, CP1, CPz, CP3, CP4, CP6, T5, P3, Pz, P4, T6, PO3, PO4, O1, Oz, O2. The montage was referenced to auricular electrodes, which were linked after placing a resistor in series with each lead to compensate for any imbalance in impedance between the two auricular electrodes; the ground electrode was placed between Fz and Cz. Electrode impedance was monitored at the beginning and the end of each measurement and remained below 5 KΩ. The signal was amplified by a 40-channel EEG device (Galileo MIZAR-sirius, EBNeuro, Florence, Italy). Data was collected with a sampling rate of 4096 Hz and hardware EEG filters were set at 0.099 Hz hi-pass and 0.45*SR (0.45×4096 Hz = 1843.2 Hz) low-pass; band-pass digital filtering between 1-900 Hz was performed before the off-line analysis.

Data Analysis

All data were re-referenced to the Fz electrode to allow comparison with the majority of HFO literature (10,12).

EEG data preprocessing

A semi-automatic Independent Component Analysis (ICA)-based procedure (18) was applied to identify and remove biological (cardiac, ocular and muscular) and non-biological (power line, instrumental noise) artefacts from the data without rejecting contaminated epochs. After artefactual ICs identification, the 'cleaned' data were obtained by retro-projecting all the ICs except the artefactual ones.

Functional Source Separation

Functional source separation [FSS - (8)] technique was used to identify and extract the cerebral sources active in the somatosensory pathways. The aim of FSS is to enhance the separation of signals of interest by exploiting some a priori knowledge on their physical properties. FSS, analogous to ICA, models the set of EEG recorded signals **X** as a linear combination of an equal number of sources **S** via a mixing matrix **A** (i.e. **X=AS**). FSS expands ICA by incorporating information available about the specific brain area or neuronal pool under study into the algorithm. A functional requirement (**R**), is included with a proper weight (λ) into the contrast function (**F**). In formula $\mathbf{F} = \mathbf{J} + \lambda\mathbf{R}$, where **J** is the statistical constraint typical of ICA. FSS identifies a single functional source at a time, building a contrast function for that source that exploits fingerprint information associated to the neuronal pool to be identified (8). In general, FSS starts from the original EEG data matrix **X** for each source, and returns one functional source (FS) with the required functional property. This scheme gives us the possibility to extract the FS that maximizes the functional behavior in agreement with the functional constraint (9,10). Similarly to previous works (9,10) we used four *ad-hoc* functional constraints to extract the brain activity of the two subcortical and two cortical nodes along the somatosensory pathways (FS_BS: brainstem, FS_Th: Thalamus, FS_S1: Primary Sensory (3b) and FS_SM: Primary Sensory-Motor (SM)) from the broad range frequency band (1-900Hz).

Functional Source Positions

The spatial distribution of the field generated by the sources identified by FSS was obtained by retro-projecting the source activity into the sensors space and used as an input for inverse-problem computation. We used an equivalent current dipole (ECD) with four concentric conductive spheres model [see routine DIPFIT2 of EEGLAB v11.0, available at http://www.sccn.ucsd.edu/eeglab], to obtain ECD positions in Talairach space and projected them on the template brain of the Montreal Neurological Institute (MNI).

LFO-SSEP – peak latency and amplitude analysis

Low Frequency Oscillation (LFO) analysis on the SSEP was obtained by applying a 1–400 Hz band-pass filter to the averaged Functional Sources (FSs). The P14, P16, N20 and P22 peak latencies and the peak amplitudes (using the P14-0, P16-0, 0-N20 and P22-0 amplitude differences) were selected subject by subject in both groups and used for the following statistical analysis.

LFO and HFO – Time frequency analysis

All time–frequency analyses were performed using a Morlet wavelet, with a constant parameter equal to seven that offered the best compromise between time and frequency resolution. Statistical significance of power changes was evaluated with a resampling bootstrap technique, and thresholded at $p = 0.01$. Non-significant changes were set to zero. LFO activities and High Frequency Oscillation (HFO) activities of each source were extracted by applying, respectively, a 1-400 Hz and a 450–750 Hz (10,12) band-pass filter to the averaged FSs.

All recordings were numbered anonymously and analyzed blindly off-line by one investigator (C.P.), who was not involved in recruitment and inclusion of subjects, as well as in the recording of the EEG.

Statistical Analysis

Preliminary descriptive analysis showed that LFO-SSEP peak latency and amplitude of the four sources had a normal distribution, whereas LFO and HFO power amplitude of the four sources had a non-normal distribution. To obtain a better approximation to a Gaussian curve, the latter were logarithmically transformed before the analysis and achieved an appropriate equivalence to a normal distribution (Kolmogorov-Smirnov test, $p > 0.2$).

A General Linear Model approach was used to analyze the "between-factor" × "two within-factor" interaction effect for LFO-SSEP peak latencies and amplitudes and LFO and HFO power amplitudes. The between-subject factor was diagnostic group (HV vs. MS); the two within-subject factors were: hemisphere (left vs. right) and source (FS_BS *vs*. FS_Th *vs*. FS_S1 *vs*. FS_SM). Two models of repeated measures ANOVA (rm-ANOVA) followed by univariate ANOVAs were used to investigate the interaction effect on LFO-SSEP peak latency and amplitude and LFO and HFO power amplitude. Univariate results were analyzed only if Wilks' Lambda multivariate significance criterion was satisfied. The sphericity of the covariance matrix was verified with the Mauchly Sphericity Test. In case of violation of the sphericity assumption, Greenhouse-Geisser (G-G) epsilon (ε) adjustment was used. Statistical significance was set at $p < 0.05$. To define which comparison(s) contributed to the major effects, post hoc tests were performed with Fisher's Least Significant Difference (LSD). We adopted the Bonferroni adjustment for multiple comparisons

(0.05 / 16; value of significance threshold divided by the number of tests presented in the interaction effect) and considered a Fisher's LSD test significant at p < 0.003125. Finally, Cohen's d, and its 95% confidence intervals (CI$_{95}$), was calculated as measure of effect size for significant post hoc test(s). Correlation analysis was carried out to search for relations among HFO power amplitudes and clinical variables (onset of migraine history; attack frequency; headache severity, measured on 0-10 visual analogue scale; attack duration, and days elapsed from the last migraine attack).

Results

The main features of the sample are presented in Table 1. The MO and the HV groups did not differ in gender ($\chi_1^2 = 0.482$, p$_{2\text{-tailed}}$ = 0.683) and age (t_{38} = -0.820, p$_{2\text{-tailed}}$ = 0.418).

Functional Source Behavior

The localization of functional sources (FSs) was consistent with the recruitment of neuronal pools at brain stem (BS) and thalamic (Th) levels (Figure 1, first row) for the subcortical generators. These were maximally activated between 14 ms and 16 ms after the stimulus in the LFO range (Figure 2 for the Left Hemisphere - LH and Figure 3 for the Right Hemisphere - RH, SEP column). Primary sensory (BA 3b or S1) and primary motor (BA4 or M1) areas (Figure 1, second row), were maximally activated between 20 and 22 ms after the stimulus in the LFO range (Figure 2 for the LH and Figure 3 for the RH, SEP column).

The LFO-SSEP time-series of all sources are shown in the time domain in the Figure 2 and Figure 3 (SEP column). At LFO-SSEP peak latencies, in both hemispheres, clear bursts of high frequency activity were presented as time-series revealed in the time domain (SEP column) and spectral properites reveled in the time frequency plots (Time Frequency column).

LFO-SEP – peak latencies and amplitudes

In the rm-ANOVA model with LFO-SSEP peak latency as dependent variable, multivariate test was not significant for the "*diagnostic group*" × "*hemisphere*" × "*source*" interaction effect (Wilks' Lambda = 0.797, F$_{3,36}$ = 2.117, p = 0.123). No significant difference emerged in LFO-SSEP peak amplitude between the two groups in both hemispheres for the four source location. Similarly, in the rm-ANOVA model with LFO-SSEP peak amplitude as dependent variable, multivariate test was not significant for the "*diagnostic group*" × "*hemisphere*" × "*source*" interaction effect (Wilks'

Lambda = 0.950, $F_{3,36}$ = 0.543, p = 0.656). Table 2 shows peak latencies and amplitudes in all the conditions.

LFO and HFO power

In the rm-ANOVA model with LFO power as dependent variable multivariate test was not significant for the "*diagnostic group*" × "*hemisphere*" × "*source*" interaction effect (Wilks' Lambda = 0.873, $F_{3,36}$ = 1.755, p = 0.173). Figure 4 shows raw data of LFO power amplitudes in all the conditions.

On the contrary, the rm-ANCOVA model with HFO power amplitude as dependent variable multivariate test showed a significant effect for the "*diagnostic group*" × "*hemisphere*" × "*source*" interaction (Wilks' Lambda = 0.620, $F_{3,36}$ = 7.344, p < 0.001). After G-G correction was applied for univatiate tests due to a violation in sphericity, univariate rm-ANOVAs for HFO power confirmed the difference between groups ($F_{3,114}$ = 3.931, ε = 0.743, p = 0.020). Post hoc tests revealed that the main contributors to the difference between MO and HV in HFO power were brain stem [left: p < 0.0001; Cohen's d (CI_{95}) = -1.16 (-1.36 – -0.94); right: p < 0.0001; Cohen's d (CI_{95}) = -1.48 (-1.70 – -1.36)] and thalamic sources [left: p < 0.0003; Cohen's d (CI_{95}) = -1.44 (-1.63 – -1.22); right: p = 0.003; Cohen's d (CI_{95}) = -0.95 (-1.15 – -0.79)]. According to conventional values of Cohen's d, the effect size could be considered as large. As shown in Figure 5 (raw data), MO had significant lower power values than HV for left and right brainstem and thalamic sources, suggesting a dysfunction of these subcortical structures. The absence of significant between groups power difference in cortical sources is not supportive of a primary dysfunction at cortical level in the somatosensory region in migraine.

Correlation analysis showed that the age of headache onset was positively correlated with HFO power amplitudes of the right brainstem (r = 0.602, p = 0.005; Figure 6A) and thalamic sources (r = 0.640, p = 0.002; Figure 6B). No other correlations resulted significant.

Discussion

The most relevant finding of this study is that evoked brainstem and thalamic high-frequency oscillatory power is bilaterally reduced in patients with MO after median nerve stimulation at the wrist. The severity of this impairment correlated with the age of onset of migraine manifestations. This spectral abnormality was not present in the two cortical sources, or in the low-frequency oscillatory activity for both subcortical and cortical sources.

The diverging behavior of HFO and LFO is not unexpected given that multichannel source localisation data and pharmacological manipulation studies have shown that LFO and HFO activities are functionally independent, and different generators within the same or nearby cortical areas have been hypothesized (19). Low-frequency activity along the somatosensory pathway represents slow postsynaptic responses, sequentially evoked during passage of each somatosensory node, and clearly confined in their corresponding anatomical location (19). HFOs on the contrary reflect more direct and very fast neuronal spike-activity with a continuous bottom-up outflow of synchronized activity (19). In animal models, dorsal column brainstem nuclei possess an intrinsic capability to generate HFO activity that synchronize with the contralateral ventroposterolateral (VPL) nucleus (20), while in humans, HFO superimposed on the dorsal column nuclei (DCN) potential were detected in intra-operatory SSEP recordings (21) or by nasopharyngeal electrode (22). The HFO extracted at the brainstem level might reflect activity of cuneothalamic projection neurons from the DCN in the pons (medial lemniscal pathway in the brainstem) (21). These nuclei are constituted by a shell and a core region, the latter is the site of the great majority of the cells project to the VPL nucleus of the contrataleral thalamus (20). It is of particular interest for migraine that, in experimental and animal models, the spinothalamic projecting neurons are reported to have branches ending in both VPL and nucleus ventralis posteromedialis (VPM) (23–25), where converges trigeminothalamic tract, and that in turn these thalamic nuclei send inputs to the region of primary somatosensory cortex processing information from the head (26), where is located the migraine pain. HFO activity within or close to the thalamus and thalamocortical fibres has been recorded in experimental models (27) and in humans during deep brain electrode implantation (21), and suggested to reflect near-field activity from the somatosensory relay thalamic nucleus. Magnetoencephalographic and electroencephalographic studies have identified two generators of HFOs, one in somatosensory area 3b and the other in neighbouring sensorimotor areas with an orthogonal orientation (see (5) for review). These cortical generators may reflect presynaptic repetitive discharges conducted in the terminal segments of thalamocortical axons and/or postsynaptic contributions from intracortical specialized very fast spiking neurons, that closely approximated the periodicity of the surface recorded HFOs as showed in animals (6) and in humans with implanted electrodes (28).

The role of HFO as intermediate phenotype in migraine patients has been explored in the last decade using the classic single channel approach. This methodology lacks the spatial accuracy necessary to resolve the contribution of subcortical and cortical regions to this phenomenon. Decreased power of early HFOs in migraine between attacks was independently reported by two groups (12,29) and explained as reflecting generic activity in thalamo-cortical afferents. Moreover, low thalamocortical drive between attacks was associated with the most pronounced cortical

neurophysiological abnormalities and a worsening in the severity of migraine clinical course, such as increase attack frequency (13), intensity and duration of the headache phase (14).

The importance of the the integrity of subcortical sources in modulating the burden of migraine is supported by our finding that right brainstem and thalamic power amplitude values correlate positively with the age of headache onset, i.e. the earlier the age of first migraine manifestation, the higher the malfunction of subcortical nodes along the somatosensory pathway. The different outcome in correlation analysis between the two sides may result from brainstem/thalamic structural asymmetries that have been previously reported by MR imaging analyses (30,31). Migraine is a functional brain disorder in which genetics plays a relevant role in setting the individual "threshold" develop migraine attacks (32). The body of evidence from population-based family studies and twin studies indicates that genetic factors account for approximately 50% in liability to MO (33) and that first-degree family members of patients affected from MO have twice the risk to develop migraine compared with the general population (34). These findings and the evidence emerging from cohort studies suggest that a genetic predisposition to migraine makes probands more susceptible to migraine earlier in life (35). Interestingly, neurophysiological studies in asymptomatic subjects with a family history of migraine reported subcortico/cortical neurophysiological abnormalities similar those seen in migraineours (36). The prevalence of these which correlated significantly with the number of migraine sufferers among 1st and 2nd degree relatives. Collectively, these observations in conjunction with the positive correlation between age of migraine onset and severity of subcortical brainstem and thalamic impairment in HFO activity strongly suggest a link between the underlying genetic load and the interictal abnormal sensory processing in migraineurs.

Relevance to migraine pathophysiology

In this study we found that low thalamic/thalamocortical drive is accompanied by equally low brainstem activation. The notion of altered brainstem monoaminergic neurotransmission in migraine has been supported by biochemical (15), neurophysiological (37), and neuroimaging (16) studies. Brain imaging studies have identified increased blood flow in the dorso-lateral part of the brainstem during attacks of migraine without aura (16). A number of studies in migraine have shown dysfunctional endogenous pain modulation at brainstem level (38–40). Altered turnover of monoaminergic neurotransmitters (serotonin, dopamine, acetylcholine, etc.) released by brainstem nuclei may also underlie aberrant brainstem pain modulation system in migraine (see for a review (15)). This was confirmed with neuroimaging focused on receptor populations expressed in the anatomical structures involved in migraine pathophysiology, including the brainstem, following the migraine cycle (16). Reduced monoaminergic, especially serotonergic, availability in the migraineur brain was claimed as possible culprit of the electrocortical abnormalities frequently

observed in migraine interictally. In fact, lack of habituation to repetitive stimuli detected with brainstem auditory evoked potentials (41) and event-related cognitive potentials (42) was found to be related to platelet serotonin content during the migraine cycle. The intensity dependence of auditory evoked potentials (IDAP) – known to be inversely related marker of synaptically released serotonin in the CNS – was found to be stronger in migraine interictally respect to healthy controls (43).

The body of evidence reviewed here seems to suggest that the pathophysiology of migraine could be driven by a complex dysfunction of brainstem and thalamocortical connectivity. A simultaneous dysfunction of thalamocortical activity and of brainstem monoaminergic nuclei is the hallmark of various functional brain disorders grouped under the name "thalamocortical dysrhythmia" (TCD) syndromes. The TCD theory proposes that a functional and anatomical dysconnection of the thalamus from the brainstem monoaminergic subcortical areas induces a change of rhythmic thalamocortical activity favouring cortical rhythms of lower frequency. This in turn is known to reduce the excitation of pyramidal cells at the beginning of the stimulus and of fast-spiking inhibitory interneurons during stimulus repetition (44). Whether this abnormal oscillatory pattern may be responsible for the symptoms that accompany migraine both ictally and, for minor extent, interictally such as photo/phophobia and vertigo, remains to be determined.

A limitation of this study is that we are not in a position to evaluate if our findings are specific to migraine or shared by other headache syndromes. To achieve this, comparative studies with other primary headache disorders are necessary.

Conclusions

In conclusion, the results from this study confirm and extend those previously obtained with the classic single channel approach. The novelty of our findings is in providing evidence that low interictal thalamic/thalamocortical drive in migraine can be due to low brainstem activation, and not to a primary cortical dysfunction. The evidence of greater impairment in subcortical HFOs in patients with earlier onset of the disease suggests a role of predisposing genetic factors in the pathophysiology of this electrophysiological intermediate phenotype. Finally, although neurophysiological procedures have not recognised as useful tools for the diagnosis of non-acute primary headache disorders (45), a more systematic application of the proposed evoked EEG analysis techniques may provide relevant indications about subcortical-cortical activity in migraine. This data can be acquired in a routine clinical setting and the procedure requires minimal patient collaboration. A prospective study could determine the value of this diagnostic procedure in supporting the decision on appropriate pharmacological and non-pharmacological treatment (46).

Acknowledgment

Figure legends

Figure 1 – Source positions

Grand average position and orientation of the ECD for Healthy Volunteers (left column) and Migraine patients (right column) for the four sources (FS_BS, green; FS_Th, blue; FS_S1, red and FS_SM, Magenta) superimposed on the MNI brain template in axial, coronal, and sagittal views for the left and right hemisphere. For each source in both groups talairach (x,y,z) coordinates are also shown.

Figure 2 – Source behaviours Left Hemisphere

For the grand average on the Left Hemisphere, Topographic map (Topography), Somatosensory Evoked Potential (SSEP) and High Frequency Oscillation spectral analysis (Time Frequency) for the four Functional Sources (FS_BS, green, first row; FS_Th, blue, second row; FS_S1, red, third row and FS_SM, magenta, fourth row) respectively.

Figure 3 – Source behaviours Right Hemisphere

As figure 2 but for the right hemisphere.

Figure 4 – LFO power amplitude

The means and CI_{95} of LFO power amplitudes of the four sources in both hemispheres in both groups.

Figure 5 – HFO power amplitude

The means and CI_{95} of HFO power amplitudes of the four sources in both hemispheres in both groups.

Figure 6 – Migraine onset and the HFO power activities correlation

Graphs depict the correlation between migraine onset and the HFO activities in the right BS and Th. In the graphs, continuous line is the fitting line and dotted lines show the regression bands of CI_{95} for mean.
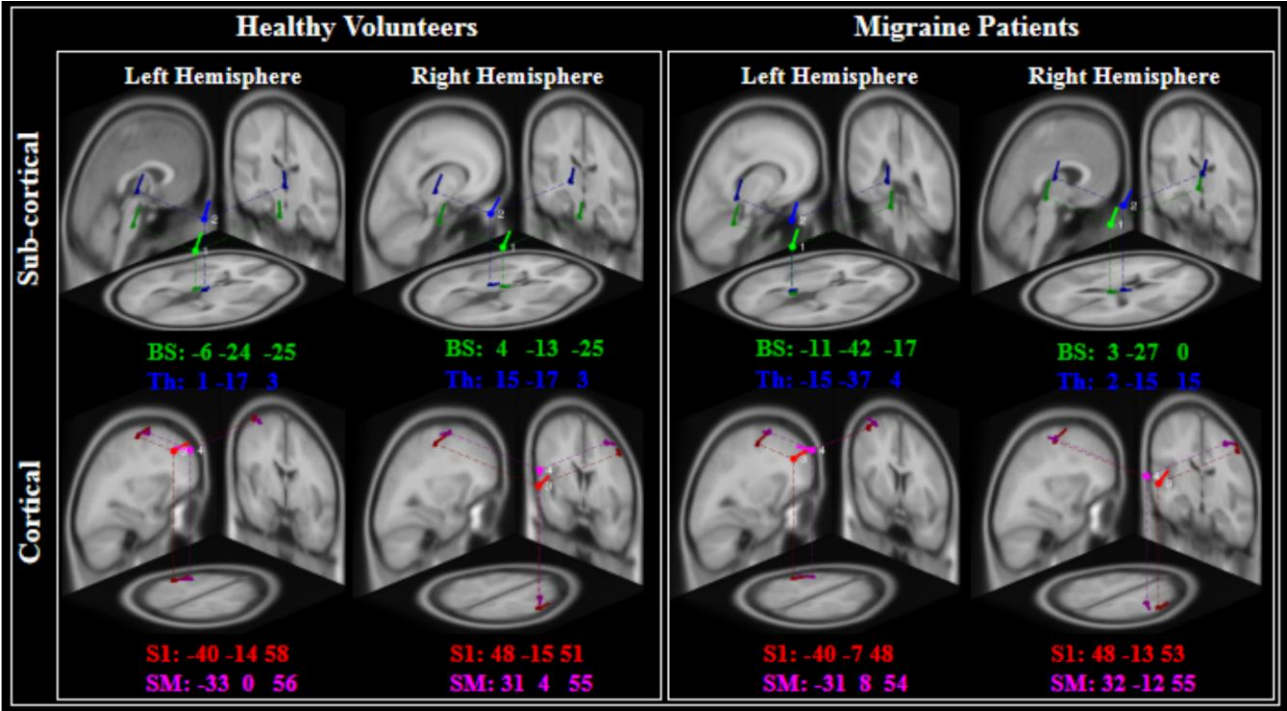
Figure 1 – Source positions
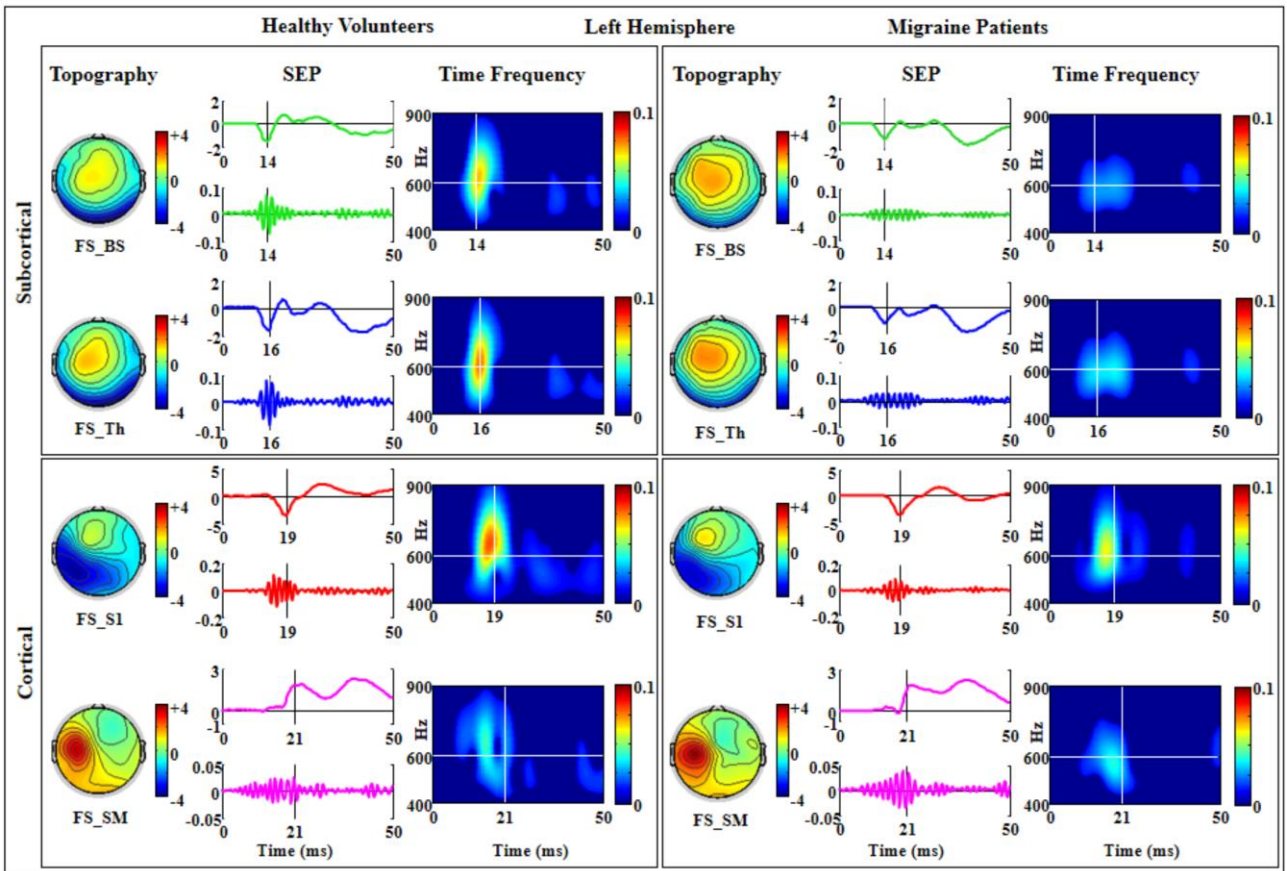

Figure 2 – Source behaviours Left Hemisphere

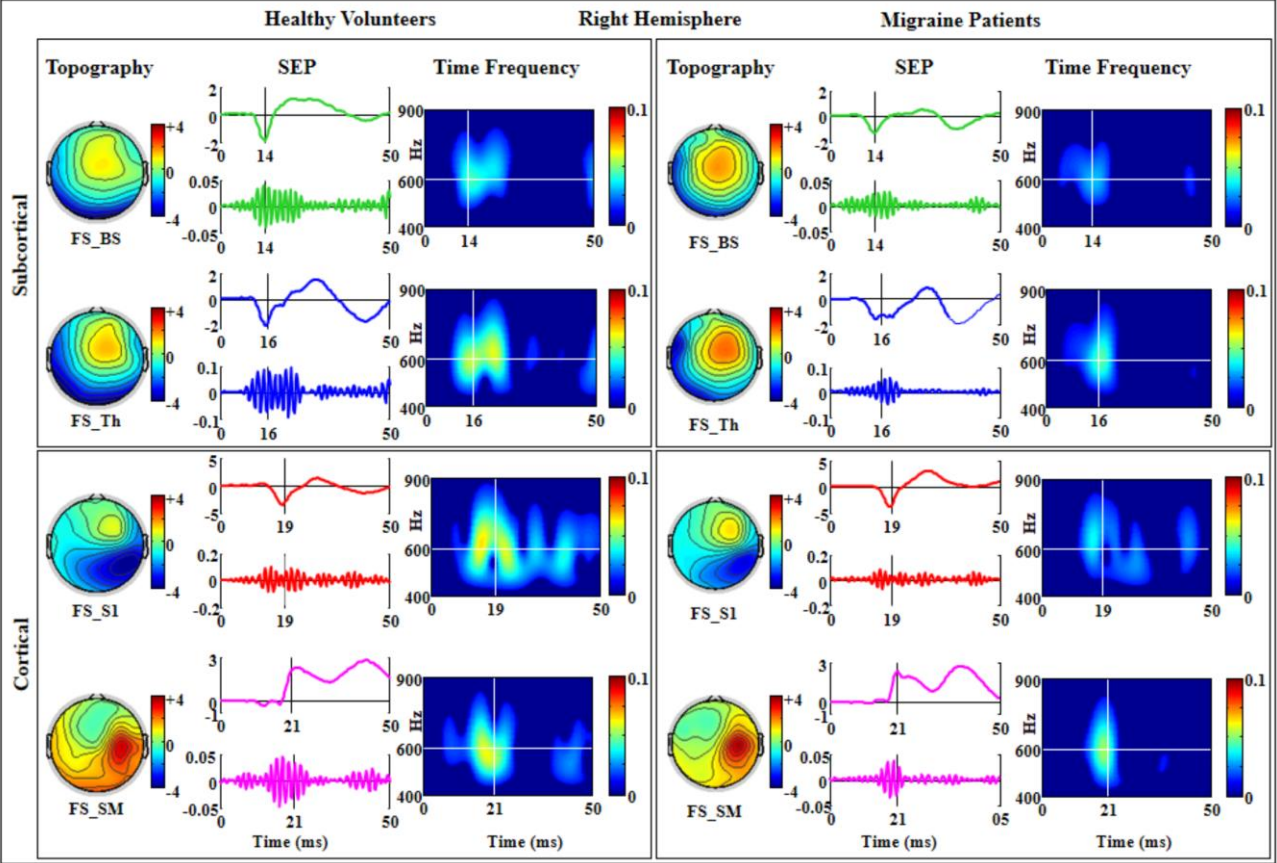**Figure 3 – Source behaviours Right Hemisphere**

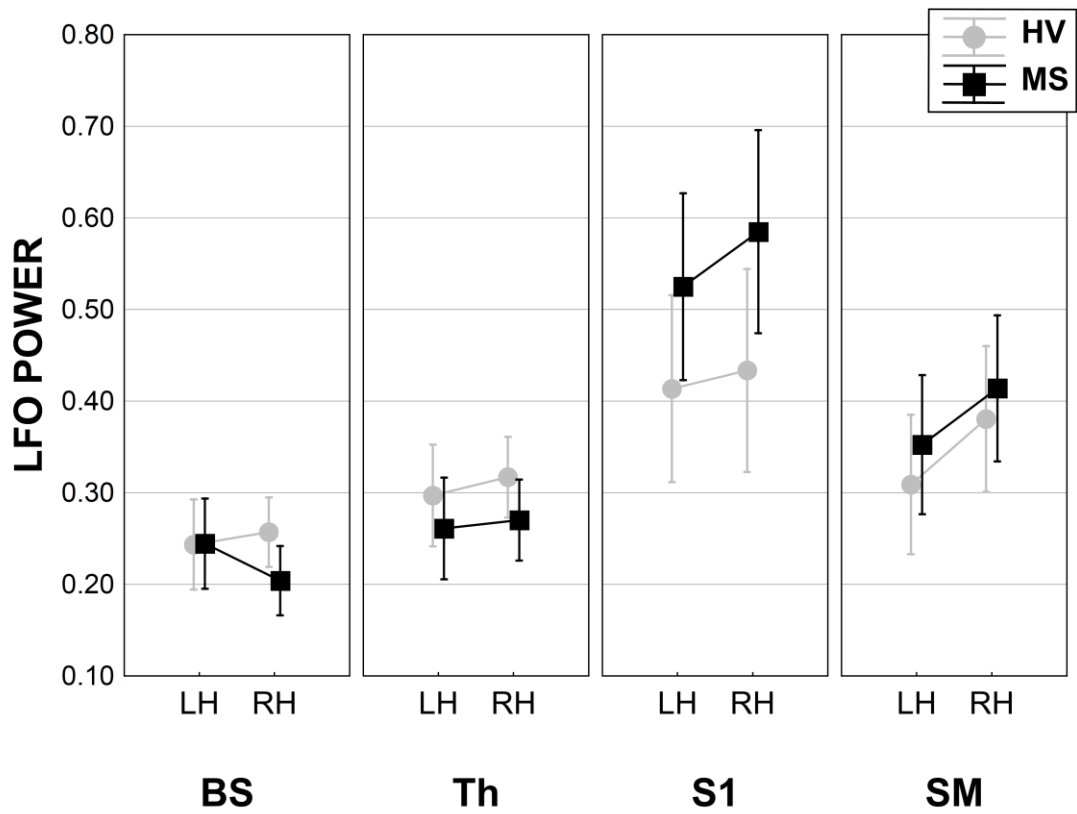

Figure 4 – LFO power amplitude

Figure 5 – HFO power amplitude

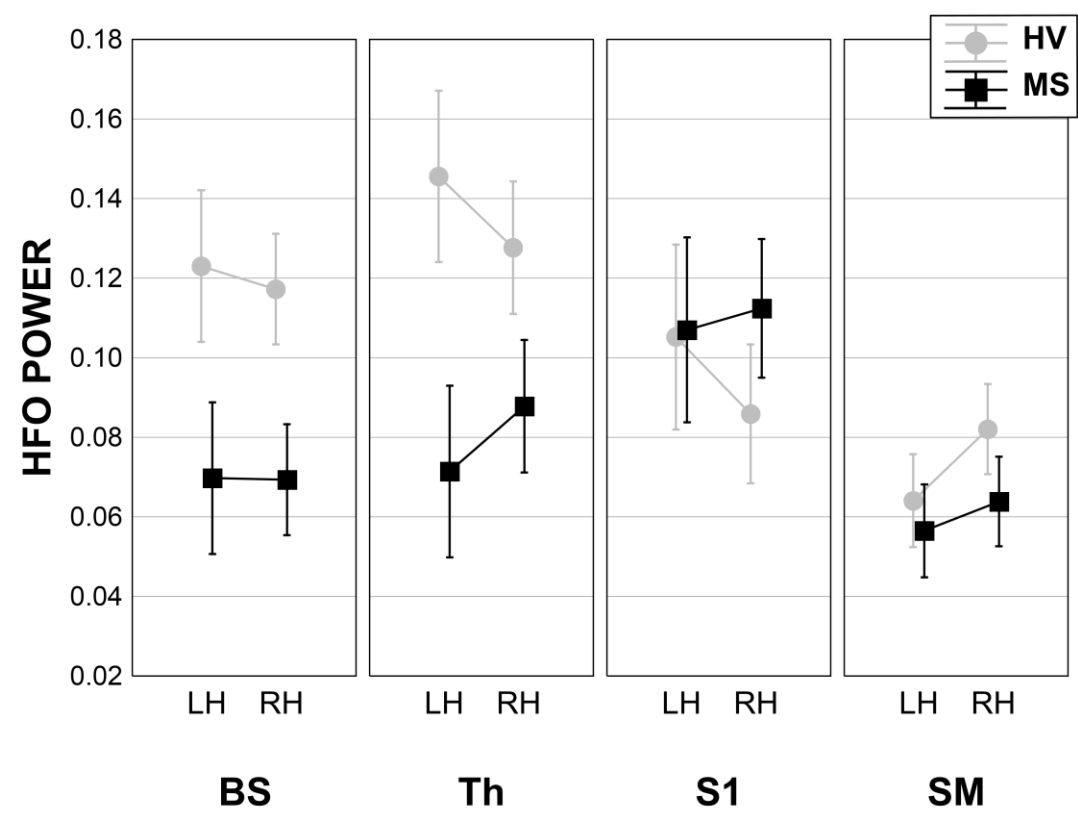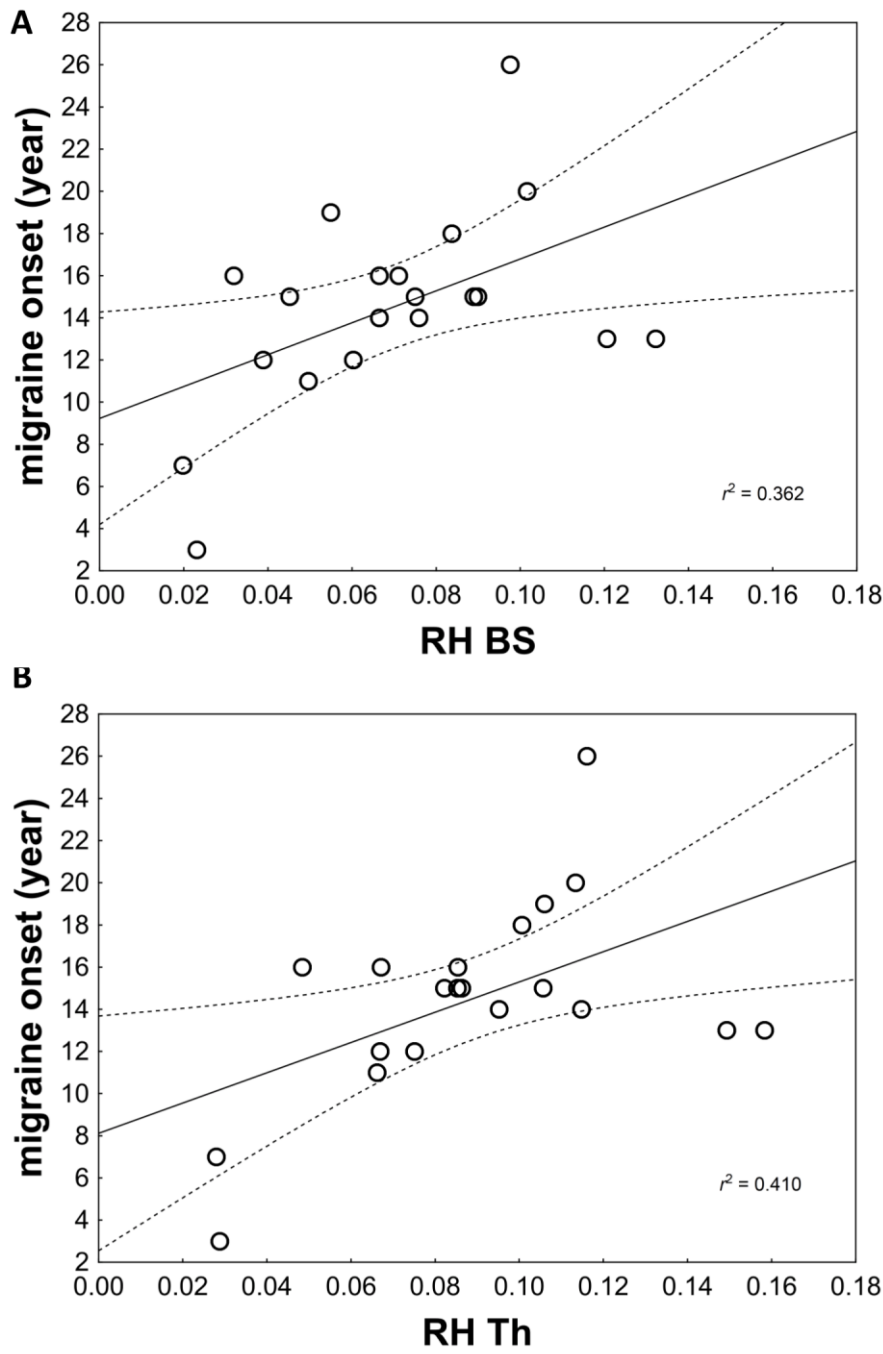**Figure 6 – Migraine onset and the HFO power activities correlation**

Article Highlights

- Morpho-functional evidence suggests that thalamus plays an important role in migraine.
- We report that reduced interictal thalamocortical drive in migraine is due to low brainstem activation, not to primary cortical dysfunction.
- The age of onset of the headache is positively correlated with high frequency oscillation power in the right brainstem and thalamus.
- We propose that functional and anatomical thalamic dysconnection from the brainstem can contribute to migraine attacks recurrence.

References

1. Burstein R, Jakubowski M, Garcia-Nicas E, Kainz V, Bajwa Z, Hargreaves R, et al. Thalamic sensitization transforms localized pain into widespread allodynia. *Ann Neurol*. 2010;68:81–91.

2. Noseda R, Kainz V, Jakubowski M, Gooley JJ, Saper CB, Digre K, et al. A neural mechanism for exacerbation of headache by light. *Nat Neurosci*. 2010;13:239–45.

3. Coppola G, Tinelli E, Lepre C, Iacovelli E, Di Lorenzo C, Di Lorenzo G, et al. Dynamic changes in thalamic microstructure of migraine without aura patients: a diffusion tensor magnetic resonance imaging study. *Eur J Neurol*. 2014;21:287–e13.

4. Magon S, May A, Stankewitz A, Goadsby PJ, Tso AR, Ashina M, et al. Morphological Abnormalities of Thalamic Subnuclei in Migraine: A Multicenter MRI Study at 3 Tesla. *J Neurosci*. 2015;35:13800–6.

5. Curio G. Linking 600-Hz "spikelike" EEG/MEG wavelets ("sigma-bursts") to cellular substrates: concepts and caveats. *J Clin Neurophysiol*. 2000;17:377–96.

6. Baker SN, Curio G, Lemon RN. EEG oscillations at 600 Hz are macroscopic markers for cortical spike bursts. *J Physiol*. 2003;550:529–34.

7. Restuccia D, Valeriani M, Grassi E, Mazza S, Tonali P. Dissociated changes of somatosensory evoked low-frequency scalp responses and 600 Hz bursts after single-dose administration of lorazepam. *Brain Res*. 2002;946:1–11.

8. Tecchio F, Porcaro C, Barbati G, Zappasodi F. Functional source separation and hand cortical representation for a brain-computer interface feature extraction. *J Physiol*. 2007;580:703–21.

9. Porcaro C, Coppola G, Di Lorenzo G, Zappasodi F, Siracusano A, Pierelli F, et al. Hand somatosensory subcortical and cortical sources assessed by functional source separation: an EEG study. *Hum Brain Mapp*. 2009 [cited 2016 Feb 7];30:660–74.

10. Porcaro C, Coppola G, Pierelli F, Seri S, Di Lorenzo G, Tomasevic L, et al. Multiple frequency functional connectivity in the hand somatosensory network: an EEG study. *Clin Neurophysiol*. 2013;124:1216–24.

11. Coppola G, Iacovelli E, Bracaglia M, Serrao M, Di Lorenzo C, Pierelli F. Electrophysiological correlates of episodic migraine chronification: evidence for thalamic involvement. *J Headache Pain*. 2013;14:76.

12. Coppola G, De Pasqua V, Pierelli F, Schoenen J. Effects of repetitive transcranial magnetic stimulation on somatosensory evoked potentials and high frequency oscillations in migraine. *Cephalalgia*. 2012;32:700–9.

13. Restuccia D, Vollono C, Del P, Martucci L, Zanini S. Somatosensory High Frequency Oscillations reflect clinical fluctuations in migraine. *Clin Neurophysiol*. 2012;123:2050–6.

14. Coppola G, Bracaglia M, Di Lenola D, Iacovelli E, Di Lorenzo C, Serrao M, et al. Lateral inhibition in the somatosensory cortex during and between migraine without aura attacks: correlations with thalamocortical activity and clinical features. *Cephalalgia*. 2015;in press.

15. Hamel E. Serotonin and migraine: biology and clinical implications. *Cephalalgia*. 2007;27:1293–300.

16. Sprenger T, Borsook D. Migraine changes the brain: neuroimaging makes its mark. *Curr Opin Neurol*. 2012;25:252–62.

17. Cosentino G, Fierro B, Brighina F. From different neurophysiological methods to conflicting pathophysiological views in migraine: A critical review of literature. *Clin Neurophysiol*. 2014;125:1721–30.

18. Barbati G, Porcaro C, Zappasodi F, Rossini PM, Tecchio F. Optimization of an independent component analysis approach for artifact identification and removal in magnetoencephalographic signals. *Clin Neurophysiol*. 2004;115:1220–32.

19. Gobbelé R, Waberski TD, Simon H, Peters E, Klostermann F, Curio G, et al. Different origins of low- and high-frequency components (600 Hz) of human somatosensory evoked potentials. *Clin Neurophysiol*. 2004;115:927–37.

20. Canedo A, Martinez L, Mariño J. Tonic and bursting activity in the cuneate nucleus of the chloralose-anesthetized cat. *Neuroscience*. 1998;84:603–17.

21. Insola A, Padua L, Mazzone P, Scarnati E, Valeriani M. Low and high-frequency somatosensory evoked potentials recorded from the human pedunculopontine nucleus. *Clin Neurophysiol*. 2014;125:1859–69.

22. Restuccia D, Della M, Valeriani M, Rubino M, Scarano E, Tonali P. Brain-stem components of high-frequency somatosensory evoked potentials are modulated by arousal changes: nasopharyngeal recordings in healthy humans. *Clin Neurophysiol*. 2004;115:1392–8.

23. Boivie J. Thalamic projections from lateral cervical nucleus in monkey. A degeneration study. *Brain Res*. 1980;198:13–26.

24. Yokota T, Koyama N, Matsumoto N. Somatotopic distribution of trigeminal nociceptive neurons in ventrobasal complex of cat thalamus. *J Neurophysiol*. 1985;53:1387–400.

25. Craig AD. Distribution of trigeminothalamic and spinothalamic lamina I terminations in the macaque monkey. *J Comp Neurol*. 2004;477:119–48.

26. Cerkevich CM, Qi H-X, Kaas JH. Thalamic input to representations of the teeth, tongue, and face in somatosensory area 3b of macaque monkeys. *J Comp Neurol*. 2013;521:3954–71.

27. Steriade M, Curró Dossi R, Contreras D. Electrophysiological properties of intralaminar thalamocortical cells discharging rhythmic (approximately 40 HZ) spike-bursts at approximately 1000 HZ during waking and rapid eye movement sleep. *Neuroscience*. 1993;56:1–9.

28. Barba C, Valeriani M, Colicchio G, Tonali P, Restuccia D. Parietal generators of low- and high-frequency MN (median nerve) SEPs: data from intracortical human recordings. *Clin Neurophysiol*. 2004;115:647–57.

29. Sakuma K, Takeshima T, Ishizaki K, Nakashima K. Somatosensory evoked high-frequency oscillations in migraine patients. *Clin Neurophysiol*. 2004;115:1857–62.

30. Fabiano AJ, Horsfield MA, Bakshi R. Interhemispheric asymmetry of brain diffusivity in normal individuals: a diffusion-weighted MR imaging study. *AJNRAmerican J Neuroradiol*. 2005;26:1089–94.

31. Lambert C, Lutti A, Helms G, Frackowiak R, Ashburner J. Multiparametric brainstem segmentation using a modified multivariate mixture of Gaussians. *NeuroImage Clin*. 2013;2:684–94.

32. Di Lorenzo C, Grieco GS, Santorelli FM. Migraine headache: a review of the molecular

genetics of a common disorder. *J Headache Pain*. 2012 [cited 2016 Mar 1];13:571–80.

33. Ziegler DK, Hur YM, Bouchard TJ, Hassanein RS, Barter R. Migraine in twins raised together and apart. *Headache*. 1998;38:417–22.

34. Russell MB, Olesen J. Increased familial risk and evidence of genetic factor in migraine. *BMJ (Clinical Res ed)*. 1995;311:541–4.

35. Eidlitz-Markus T, Haimi-Cohen Y, Zeharia A. Association of age at onset of migraine with family history of migraine in children attending a pediatric headache clinic: a retrospective cohort study. *Cephalalgia*. 2015;35:722–7.

36. Siniatchkin M, Kropp P, Gerber WD. Contingent negative variation in subjects at risk for migraine without aura. *Pain*. 2001;94:159–67.

37. Coppola G, Di Lorenzo C, Schoenen J, Pierelli F. Habituation and sensitization in primary headaches. *J Headache Pain*. 2013;14:65.

38. de Tommaso M, Difruscolo O, Sardaro M, Libro G, Pecoraro C, Serpino C, et al. Effects of remote cutaneous pain on trigeminal laser-evoked potentials in migraine patients. *J Headache Pain*. 2007 [cited 2016 Mar 3];8:167–74.

39. Coppola G, Currà A, Serrao M, Di Lorenzo C, Gorini M, Porretta E, et al. Lack of cold pressor test-induced effect on visual-evoked potentials in migraine. *J Headache Pain*. 2010;11:115–21.

40. Nahman-Averbuch H, Granovsky Y, Coghill RC, Yarnitsky D, Sprecher E, Weissman-Fogel I. Waning of "conditioned pain modulation": a novel expression of subtle pronociception in migraine. *Headache*. 2013;53:1104–15.

41. Sand T, Zhitniy N, White LR, Stovner LJ. Brainstem auditory-evoked potential habituation and intensity-dependence related to serotonin metabolism in migraine: A longitudinal study. *Clin Neurophysiol*. 2008;119:1190–200.

42. Evers S, Quibeldey F, Grotemeyer KH, Suhr B, Husstedt IW. Dynamic changes of cognitive habituation and serotonin metabolism during the migraine interval. *Cephalalgia*. 1999;19:485–91.

43. Ambrosini A, Rossi P, De Pasqua V, Pierelli F, Schoenen J. Lack of habituation causes high intensity dependence of auditory evoked cortical potentials in migraine. *Brain*. 2003;126:2009–15.

44. Llinás RR, Steriade M. Bursting of thalamic neurons and states of vigilance. *J Neurophysiol*. 2006;95:3297–308.

45. Sandrini G, Friberg L, Coppola G, Jänig W, Jensen R, Kruit M, et al. Neurophysiological tests and neuroimaging procedures in non-acute headache (2nd edition). *Eur J Neurol*. 2011;18:373–81.

46. Coppola G, Di Lorenzo C, Serrao M, Parisi V, Schoenen J, Pierelli F. Pathophysiological targets for non-pharmacological treatment of migraine. *Cephalalgia*. 2015; doi: 10.1177/0333102415620908